

Seasonal variation in apparent conductivity and soil salinity at two Narragansett Bay, RI salt marshes

Richard McKinney^{Corresp., 1}, Alana Hanson¹, Roxanne Johnson¹, Michael Charpentier²

¹ Atlantic Ecology Division, US Environmental Protection Agency, Narragansett, Rhode Island, United States

² SRA International Inc., Narragansett, Rhode Island, United States

Corresponding Author: Richard McKinney
Email address: Mckinney.Rick@epa.gov

Measurement of the apparent conductivity of salt marsh sediments using electromagnetic induction (EMI) is a rapid alternative to traditional methods of salinity determination that can be used to map soil salinity across a marsh surface. Soil salinity measures can provide information about marsh processes, since salinity is important in determining the structure and function of tidally influenced marsh communities. While EMI has been shown to accurately reflect salinity to a specified depth, more information is needed on the potential for spatial and temporal variability in apparent conductivity measures that may impact the interpretation of salinity data. In this study we mapped soil salinity at two salt marshes in the Narragansett Bay, RI estuary monthly over the course of several years to examine spatial and temporal trends in marsh salinity. Mean monthly calculated salinity was 25.8 ± 5.5 ppt at Narrow River marsh (NAR), located near the mouth of the Bay, and 17.7 ± 5.3 ppt at Passeonkquis marsh (PAS) located in the upper Bay. Salinity varied seasonally with both marshes, showing the lowest values (16.3 and 8.3 ppt, respectively) in April and highest values (35.4 and 26.2 ppt, respectively) in August. Contour plots of calculated salinities showed that while the mean whole-marsh calculated salinity at both sites changed over time, within-marsh patterns of higher versus lower salinity were maintained at NAR but changed over time at PAS. Calculated salinity was significantly negatively correlated with elevation at NAR during a sub-set of 12 sample events, but not at PAS. Best-supported linear regression models for both sites included one-month and 6-month cumulative rainfall, and tide state as potential factors driving observed changes in calculated salinity. Mapping apparent conductivity of salt marsh sediments may be useful both identifying within-marsh micro-habitats, and documenting marsh-wide changes in salinity over time.

1

2 **Seasonal variation in apparent conductivity and soil**
3 **salinity at two Narragansett Bay, RI salt marshes**

4

5 Richard A. McKinney¹, Alana R. Hanson¹, Roxanne L. Johnson¹, Michael A. Charpentier²

6

7 ¹US Environmental Protection Agency, Atlantic Ecology Division, Narragansett, RI USA

8 ²SRA International Inc., Narragansett, RI USA

9

10 Corresponding Author:

11 Richard A. McKinney

12 US EPA, 27 Tarzwell Drive, Narragansett, RI 02882 USA

13 Email address: mckinney.rick@epa.gov

14

15

16 Abstract

17

18 Background

19 Measurement of the apparent conductivity of salt marsh sediments using electromagnetic
20 induction (EMI) is a rapid alternative to traditional methods of salinity determination that can be
21 used to map soil salinity across a marsh surface. Soil salinity measures can provide information
22 about marsh processes, since salinity is important in determining the structure and function of
23 tidally influenced marsh communities. While EMI has been shown to accurately reflect salinity
24 to a specified depth, more information is needed on the potential for spatial and temporal
25 variability in apparent conductivity measures that may impact the interpretation of salinity data.

26 Methods

27 We used EMI to map soil salinity at two salt marshes in the Narragansett Bay, RI estuary
28 monthly over the course of several years to examine spatial and temporal trends in marsh
29 salinity. A portable conductivity meter was used to generate apparent conductivity values along
30 randomly-oriented transects across the marsh surface, which were then calibrated with traditional
31 porewater salinity measures taken at a randomly selected sub-set of sample points and converted
32 to salinity values. Data were stored in a shapefile and subsequently used to create contour maps
33 of salinity across the marsh surface.

34 Results

35 Mean monthly calculated salinity was 25.8 ± 5.5 ppt at Narrow River marsh (NAR), located near
36 the mouth of the Bay, and 17.7 ± 5.3 ppt at Passeonkquis marsh (PAS) located in the upper Bay.
37 Salinity varied seasonally with both marshes, showing the lowest values (16.3 and 8.3 ppt,
38 respectively) in April and highest values (35.4 and 26.2 ppt, respectively) in August. Contour
39 plots of calculated salinities showed that while the mean whole-marsh calculated salinity at both

40 sites changed over time, within-marsh patterns of higher versus lower salinity were maintained at
41 NAR but changed over time at PAS. Calculated salinity was significantly negatively correlated
42 with elevation at NAR during a sub-set of 12 sample events, but not at PAS. Best-supported
43 linear regression models for both sites included one-month and 6-month cumulative rainfall, and
44 tide state as potential factors driving observed changes in calculated salinity. Mapping apparent
45 conductivity of salt marsh sediments may be useful both identifying within-marsh micro-
46 habitats, and documenting marsh-wide changes in salinity over time.

47 **Introduction**

48 Salt marshes are productive ecosystems that by nature of their position in the landscape are
49 subject to many natural and anthropogenic stressors. In the Northeast US there is concern about
50 the impact of accelerated sea level rise on salt marsh hydrology (e.g., Watson et al. 2017), and
51 how changes in marsh flooding might impact vegetation community structure (Smith et al.
52 2017). Changes in vegetation communities may impact ecosystem services provided by salt
53 marshes, and hence may have implications for their conservation and role in coastal
54 ecosystems. For example, plant community structure can influence belowground biomass
55 accumulation, which in northeastern US salt marshes is an important mechanism for marsh
56 accretion that can mitigate the effects of sea-level rise (Bricker-Urso et al. 1989, Turner et al.
57 2000). Alteration of vegetation community structure may also impact the provision of other
58 ecosystem services such as nutrient storage, habitat availability for fauna, and fisheries
59 production (Kelleway et al. 2017).

60 Tidal inundation is an important determinant of salt marsh vegetation community structure,
61 realized in part through the species-specific differences in physiological responses of plants to
62 salinity. As sea level rises the extent of tidal inundation will increase, potentially altering the
63 distribution of plant species across a marsh. Since increased inundation will alter soil porewater

64 salinity, and the primary route of water uptake in salt marsh plants is through porewater (e.g., Al
65 Hassan et al. 2017), measurement of soil porewater salinity could provide insight into potential
66 vegetation community changes resulting from sea-level rise (Silvestri and Marani 2004).
67 However, few studies have examined whole-marsh porewater salinity, in part because of the
68 labor-intensive sampling required and the difficulty in consistently obtaining porewater samples
69 at depth. An alternative is to estimate salt marsh porewater salinity by measuring the apparent
70 conductivity (EC_a) of salt marsh sediments using electromagnetic induction. This approach
71 provides estimates of soil salinity at many points in a marsh even in the absence of available
72 porewater, and can be used to gather sufficient data over the course of several hours to map soil
73 salinity across a marsh surface.

74 Measurement of EC_a in soils has been used since the mid-20th century to aid in mineral and
75 petroleum exploration and extraction, and over the past 40 years to characterize the salinity of
76 agricultural soils (DeJong et al. 1979). More recently the emergence of portable instrumentation
77 capable of rapid field measurements has allowed for its use in the estimation of other soil
78 parameters (Robinson et al. 2004). In simplest terms, at a given temperature EC_a is primarily
79 influenced by four characteristics: soil composition, i.e, mineral or clay content; bulk density;
80 moisture content; and ion concentrations, which can be representative of soil salinity (Corwin
81 and Lesch 2005). Each of these characteristics affects the bulk conductivity of soils, which in
82 turn influences the extent to which an induced electromagnetic field can be generated through the
83 soil. EC_a is determined by measuring this induced electromagnetic field, which in turn reflects
84 the average conductivity, influenced by all soil characteristics, over a volume of soil (Doolittle et
85 al. 2001). Differences in instrument response can be experimentally calibrated to changes in a

86 selected soil characteristic, allowing, under the assumption that all other characteristics are
87 constant, for a proxy measure of changes in that characteristic in the soil.

88 Application of EC_a measures in salt marshes to map soil porewater salinity was first explored in
89 the early 2000s (Paine et al. 2004) but later developed by Moore et al. (2011). The approach
90 uses an EMI instrument to measure EC_a at a series of sample points across a marsh surface. At a
91 subset of sample points, EC_a is calibrated with soil porewater salinity, measured using a sipper
92 technique (Portnoy and Valiela 1997). The resulting calibration curve is then used to calculate
93 salinity based solely on EC_a , which can then be mapped in a GIS to develop contours of salinity
94 values across the marsh surface. This technique has been used to examine the relationship
95 between plant species distribution and soil salinity during the growing season, but to our
96 knowledge no earlier studies have looked at inter-annual changes in soil salinity patterns. In this
97 study, we measured EC_a across two southern New England salt marshes along an estuarine
98 salinity gradient over a period of 2 years to investigate intra-marsh variability in soil salinity, as
99 well as potential drivers of seasonal changes in mean salinity observed at each marsh. The
100 underlying assumption of this technique is that in uniformly saturated soils, such as those found
101 in salt marshes, the contribution of soil moisture content to EC_a will be constant, and that
102 variability contributed by other soil characteristics is limited, such that changes in EC_a values
103 will accurately reflect changes in porewater salinity. To begin to evaluate the validity of this
104 assumption, we also examined changes in the relationship of EC_a and measured porewater
105 salinity at our sites with respect to potentially confounding factors such as bulk density and
106 percent moisture of the soil, and marsh elevation. Our results will provide information about the
107 magnitude of seasonal salinity change observed at a marsh, as well as identify potential drivers
108 of that change. Our study will also aid in evaluating EC_a as a surrogate for porewater salinity,

109 provide insight into potential factors influencing EC_a in salt marsh soils, and help identify
110 environmental factors that could confound the relationship between EC_a and salinity. This
111 information may allow for more widespread application of the technique, for example to use in
112 monitoring the trajectory of marsh degradation or recovery during salt marsh restoration efforts.

113 **Materials & Methods**

114

115 **Site Descriptions**

116 The study area was two salt marshes sites located in the Narragansett Bay estuary, Rhode Island,
117 USA (Figure 1). The southern site (NAR) was near the mouth of the Pettaquamscutt sub-estuary
118 ($41^{\circ} 26' 49.6''N$, $71^{\circ} 26' 58.0''W$), and had a total area of 5.89 ha. The upland edge of the site
119 was bordered by an equal proportion of private residences and forest habitat. The marsh surface
120 consisted of low marsh habitat dominated by short form *Spartina alterniflora*, and high marsh
121 habitat dominated by *Spartina patens*, *Distichlis spicata*, and *Juncus gerardii*. The high marsh –
122 upland border consisted primarily of *Iva frutescens*, and small patches of *Typha spp* and *Scirpus*
123 *spp*. The northern site (PAS) was within the Passeonkquis Cove sub-estuary ($41^{\circ} 44' 52.8''N$, 71°
124 $23' 5.2''W$), and had a total area of 2.35 ha. The upland edge of the site was bordered by an
125 approximately 100m-wide patch of trees and dense understory vegetation, transitioning to dense
126 residential land use. The marsh surface consisted of low marsh habitat dominated by tall form
127 *Spartina alterniflora*, and high marsh habitat dominated by *Spartina patens* and *Distichlis*
128 *spicata*. The high marsh – upland border consisted primarily of *Iva frutescens*, with a 0.68 ha
129 patch of *Typha spp*. at the northern edge of the border.

130 **Field Measurements**

131 A Geonics Model EM38-MK 2 Conductivity Meter (Geonics Ltd, Mississauga, Ontario, Canada)
132 was used in horizontal mode, held 50 cm over the marsh surface, to record EC_a readings. The

133 readings were the result of an induced current generated by the instrument through a maximum
134 penetration depth of approximately 1.0 m of soil at randomly distributed sample points across
135 each marsh surface. EC_a values in milliSeimans meter⁻¹ ($mS\ m^{-1}$) along with the latitude and
136 longitude of the sample point and vegetation characteristics were entered into an ArcGIS
137 shapefile using ArcPad software (ESRI, Redlands, CA) on a Trimble Nomad hand-held field
138 computer (Trimble Navigation Ltd., Sunnyvale, CA USA). Samples were taken approximately
139 every 30 days beginning October, 2015 through October 2017 ($n = 24$ sample events). Both sites
140 were surveyed on the same day at approximate 10:00 am (NAR site) and 12:00 pm (PAS site).
141 The surveys consisted of a random transect pattern walked across the marsh surface, with EC_a
142 values, vegetation characteristics, and sample point position recorded approximately every 5 m.
143 Porewater salinity measures were taken at a randomly selected sub-set of sample points using a
144 sipper consisting of a 0.5 m long piece of 1.0 mm diameter serrated metal tubing inserted in the
145 soil to a depth of 0.25 m. Once inserted, approximately 25 ml of porewater was withdrawn and
146 its salinity measured using a refractometer. Porewater salinity readings, when taken, were also
147 stored in the ArcGIS shapefile.

148 Following field sampling, shapefiles were transferred to a GIS where contour maps of calculated
149 salinity across each marsh surface were created using the ArcGIS version 10.3 Spatial Data
150 Analyst, inverse distance-weighted interpolation function (ESRI, Redlands, CA). EC_a data were
151 first converted to calculated salinity values using marsh and survey-specific calibration curves
152 constructed from a least-squares regression of EC_a values and measured porewater salinities.
153 Calculated salinity values were then used in the ArcGIS software inverse distance-weighted
154 interpolation function to create marsh-specific contour maps for each sample event.

155 Elevation values were collected using an RTK GPS Global Navigation Satellite System (GNSS)
156 receiver (Trimble Navigation Limited, Dayton, Ohio) at approximately 100 locations per marsh.
157 Each sample location was selected at approximately 5 m intervals along randomly-placed
158 transects across the marsh surface. Elevations were referenced to nearby benchmarks, and the
159 WGS84 ellipsoid model was used to determine vertical and horizontal position. The National
160 Geodetic Survey Geoid 12A (CONUS) model was used to calculate elevations from orthometric
161 heights (North American Vertical Datum of 1988 [NAVD88]), and all points were projected to
162 North American Datum of 1983 (NAD83) Universal Transverse Mercator zone 19. Digital
163 elevation models (DEMs) were created from survey points using the inverse distance weighting
164 function in ArcGIS software. Elevation values corresponding to sample point locations were
165 interpolated from the DEMs for 12 sample events corresponding to maxima and minima values
166 of mean whole-marsh calculated salinity. Three sample events were chosen to bracket each of
167 two occurrences of maxima and minima over the course of the study. Interpolated elevations
168 ranged from 0.24 – 0.76 m above mean sea level (MSL) for NAR, and from 0.49 – 1.04 ft above
169 MSL for PAS. We estimated bulk density and moisture content of soil by collecting 6 soil cores
170 of 25 cm depth along a randomly-placed transect from the upland to seaward edge at each site.
171 Two cores were collected at the mid-point of the high and low marsh zones as determined by
172 dominant plant species, and at the mid-point of the transect (mid marsh). Each core was
173 sectioned in 5 cm increments and a soil subsample from each depth was weighed, dried, and then
174 re-weighed to determine bulk density and percent moisture.

175 Total rainfall was obtained from the NOAA National Centers for Environmental Information,
176 Climate Data Online website (<https://www.ncdc.noaa.gov/cdo-web/>) for the stations Kingston,
177 RI (41° 29' 25.1"N, 71° 32' 34.8"W), located approximately 9 km northwest of NAR, and

178 Providence, RI (41° 50' 33.7"N, 71° 23' 6.7"W), located approximately 10.5 km north of PAS.
179 Daily rainfall amounts were aggregated into cumulative amounts over 24 hr, 36 hr, 1 month, 3
180 month, and 6 month periods prior to each sample event. Using Spearman Rank Correlation
181 analysis we found that 24 hr and 36 hr values were significantly correlated ($r^2 = 0.88$, $p = 0.001$),
182 as were 1 month and 3 month cumulative values ($r^2 = 0.45$, $p = 0.001$). We therefore included
183 only 24 hr, 1 month, and 6 month cumulative rainfall in our models. Tide heights were obtained
184 using online tide charts containing the time of low and high tides and corresponding tide heights
185 relative to mean low water (NOAA Tides and Currents, <https://tidesandcurrents.noaa.gov/>). We
186 used data from sites at Narragansett Pier, RI (41° 25' 56.0"N, 71° 27' 25.2"W) located
187 approximately 2 km south of NAR, and Pawtuxet Cove, RI (41° 44' 53.6"N, 71° 23' 0.6"W)
188 located approximately 1.3 km north of PAS. Tide height was extrapolated at time of sampling
189 from predicted tide ranges and expressed as a proportion of the maximum tide height for the tide
190 cycle during which the sample occurred. To indicate whether sampling occurred during a flood
191 or ebb tide, we added 1.0 to the proportions that occurred during flood tides. As a result, the
192 proportions were expressed within a range from 0.0 – 2.0, with values from 0.0 to 1.0
193 representing proportion of maximum tide height during an ebb tide, and values from 1.0 to 2.0
194 representing proportion of maximum tide height during a flood tide.

195 **Data analysis**

196 We examined temporal variability in calculated salinity for each marsh by plotting mean salinity
197 versus sample date. The effect of cumulative rainfall and tide height on mean calculated salinity
198 in the marsh was examined by constructing a series of linear regression models and evaluating
199 the models using small sample Akaike Information Criteria (AIC_c), which accounts for biases
200 that might arise from relatively small sample size (Burnham and Anderson 2002). Candidate
201 linear regression models ($n = 15$) were ranked by computing AIC_c differences or Akaike weights

202 as $\Delta AIC_c = AIC_{ci} - AIC_{cmin}$ (Burnham and Anderson, 2002, pp. 70–72). We then selected
203 models best supported by the data as having ΔAIC_c values between 0.00 and 2.00 (Burnham and
204 Anderson 2002, pp. 75–77), and calculated the relative importance ($w+(j)$) of each parameter by
205 summing the Akaike weights of all models that included this characteristic (Burnham and
206 Anderson 2002, pp. 167–169). Relative importance values provide a means to incorporate
207 selection uncertainty in the evaluation of a set of parameters, and larger values of $w+(j)$ indicate
208 whether a parameter may be a better predictor variable (Burnham and Anderson 2002).

209 Statistical analyses were performed with SAS for Windows ver. 9.41 (SAS Institute, Inc., Carey,
210 NC, USA).

211 We examined intra-marsh spatial and temporal variability in calculated salinity qualitatively by
212 visually comparing contour maps, and quantitatively by plotting calculated salinity versus
213 elevation at the sample points. We used least-squares regression of calculated salinity and
214 corresponding elevation values obtained using the DEM for a given marsh and sample event for
215 a sub-set of 12 sampling events chosen to correspond with maxima and minima in mean salinity
216 values observed over time. We then compared regression statistics to trends in overall mean
217 salinity for each marsh over time.

218 **Results**

219 Contour plots of calculated salinities showed that while the mean calculated salinity for the
220 whole marsh changed over time, patterns within marsh of higher versus lower salinity were
221 maintained for the NAR marsh, at least during the times of maximum and minimum salinity
222 (Figure 2). For example, patterns of higher salinity near the seaward edge of the marsh (right
223 hand edge of the marsh in the plot) and lower salinity towards the upland border (left hand edge
224 of the marsh in the plot) were evident both at times of maximum and minimum salinity. For
225 PAS, contour plots show a more uniform distribution of salinity values across the marsh surface,

226 particularly at calculated salinity minima (Figure 3). During the October 2017 calculated salinity
227 maximum, there was some evidence of a pattern of lower salinity towards the upland border
228 (Figure 3a, upper edge of the marsh in the plot), but that pattern was not evident during the other
229 maximum or the minima.

230 Calculated salinities for each sample event at NAR ranged from 16.3 – 35.4 ppt, with an overall
231 mean for the entire study of 25.8 ± 5.5 ppt (Table 1). Calculated salinities at PAS ranged from
232 8.3 – 26.2 ppt, with an overall mean for the entire study of 17.7 ± 5.3 ppt (Table 1). While the
233 overall mean calculated salinity showed a difference of 8.1 ppt between the two sites, for a given
234 sample event the differences varied from 0.8 – 15.8 ppt. Mean calculated salinities for both sites
235 showed maxima during the September 16, 2016 and October 27, 2017 sampling events (Figure
236 4). Mean calculated salinities showed minima during the May 4, 2016 and June 15, 2017
237 sampling events for NAR, and the May 4, 2016 and July 21, 2017 sampling events for PAS
238 (Figure 4).

239 Linear regression models of calculated salinity versus environmental factors best supported by
240 the data included one-month and 6-month cumulative rainfall and tide state for both sites (Table
241 2). At NAR, 6-month cumulative rainfall had the highest relative importance, about 1.7 times
242 that of tide state and 3 times that of one-month cumulative rainfall (Table 2). At PAS, the factors
243 6-month and one-month cumulative rainfall had essentially equivalent relative importance,
244 slightly greater than that of tidal height (Table 3).

245 The calibration coefficients for the least-squares regressions of porewater salinity versus
246 conductivity for the 24 sample events ranged from 0.13 - 0.92 at the NAR site and 0.01 - 0.75 at
247 PAS (Table 1). The coefficients were highly variable between events, without any consistent
248 patterns or trends in the values at either site.

249 Soil bulk density ranged from 0.16 – 0.34 g cm⁻³ across the two sites (Table 4) and differed
250 among marsh zones at PAS (ANOVA: df = 2, F = 7.952, p = 0.006; Tukey – Kramer test: low
251 marsh differs significantly from mid and high marsh). Soil percent moisture ranged from 69.0 –
252 84.3 % (Table 4), and, when averaged across the entire marsh, was greater at PAS (81.5 ± 3.6 %)
253 than at NAR (74.9 ± 11.5 %; t-test: df = 28; t = 2.105; p = 0.044). Percent moisture also differed
254 among zones at PAS (ANOVA: df = 2, F = 27.276, p < 0.001; Tukey – Kramer test: low marsh
255 differs significantly from mid and high marsh).

256 Calculated salinity was significantly negatively correlated with elevation at NAR during the 12
257 sample events on or around the salinity maxima and minima (Table 5). Slopes of the regression
258 equations did not differ significantly between the maximum and minimum events. Elevation at
259 NAR across all sample points during the 12 sample events ranged from 1.06 – 1.90 ft, with a
260 mean of 1.54 ft. At the PAS site, calculated salinity was significantly negatively correlated with
261 elevation for only the June and August 2017 maxima, and the October 2016 and September 2017
262 minima (Table 5). At PAS slopes of the regression equations also did not differ significantly
263 between the maximum and minimum events. Elevation at PAS across all sample points during
264 the 12 sample events ranged from 0.62 – 1.02 m, with a mean of 0.87 m.

265 **Discussion**

266 Contours of calculated salinity showed both inter- and intra-marsh differences at our sites, and
267 differences were variable over time throughout the study. At NAR, contours showed an
268 expected pattern of soil salinity with higher values near the creek edge and lower towards the
269 upland border. This pattern was generally maintained except during one period of high salinity
270 incorporating the September 16, 2016 sampling event, when overall marsh salinity was at its
271 highest. This sampling event followed a period of relatively severe drought in the region which

272 occurred from early spring through the fall of 2016. During this drought, the impact of
273 evapotranspiration on marsh hydrology may have been more pronounced and could have resulted
274 in a lower water table, and hence greater seawater influence. Several studies have modeled salt
275 marsh groundwater dynamics and water table position by considering groundwater flow as a
276 shallow, rigid aquifer in contact with a sinusoidally oscillating reservoir, and predicted the
277 potential for greater seawater inflow in the absence of groundwater inputs (Montalto et al 2007,
278 Li and Jiao 2003). Seawater influence has been shown to diminish as distance from tidal creeks
279 increases (Hemmond and Fifield 1982), but during periods of extreme drought and lowered
280 water table levels the effects of seawater inundation may be seen even in more interior portions
281 of the marsh. At PAS, intra-marsh differences were not as distinct, and the marsh often showed
282 homogeneous salinity patterns exemplified by the September 16, 2016 and July 21, 2017 sample
283 events. This may have been a result of the marsh having a relatively small surface area, or of
284 enhanced surface freshwater and groundwater inputs. Elevation increases rapidly in the upland
285 area immediately bordering the marsh, and there is a small stream bordering the western portion.
286 If the steep elevation serves to focus groundwater to the marsh, that along with the presence of
287 the stream may result in lower salinity levels during times of the year when there is little
288 evapotranspiration, and the effect may predominate over that of tidal inundation. During the
289 periods of maximum salinity, an area of the marsh near the upland border showed relatively low
290 salinity compared to those observed during the same sample events at NAR, which would further
291 support the enhanced influenced of freshwater inputs on marsh hydrology at PAS.

292 The NAR site is in the southern portion near the mouth of the Narragansett Bay estuary, and this
293 probably accounts for its measured mean whole-marsh calculated salinity being consistently
294 higher than that at PAS, which is located approximately 35 km to the north near the head of the

295 estuary. Mean surface seawater salinity at a long-term water quality sample site in Narragansett
296 Bay, located approximately 1 km north of PAS, averaged 25.1 ± 0.8 ppt, while a site
297 approximately 4 km north of NAR averaged 31.5 ± 0.2 ppt (RM, unpublished data). These
298 values should approximate the salinity of the seawater inundating each marsh during flood tides.
299 Salinity of freshwater sources would likely vary somewhat both spatially and temporally, but
300 most likely had salinities less than 5 ppt (Dodds 2002). Nothing is known of the relative
301 contribution of each salinity end-member to porewater salinity at each site, still it is likely that
302 the lower seawater salinity near PAS contributed to the lower mean calculated salinities we
303 observed.

304 Mean calculated salinities for the marshes showed maxima roughly corresponding to late
305 summer, when plant biomass is high and evapotranspiration is assumed to be at its peak, and
306 minima in early to mid-spring when evapotranspiration is low and snow melt and rainfall could
307 lead to increased freshwater input to the marshes. Several studies have suggested a conceptual
308 model of factors influencing near-surface tidal marsh porewater salinity, lower salinity
309 freshwater inputs arising from groundwater flow under the marsh and surface water inputs
310 interacting with periodic inputs of higher salinity seawater delivered during semi-diurnal flood
311 tides (Barry et al. 1996, Li and Jiao 2003, Parlange et al. 1984). Variation in the position of the
312 water table both spatially and temporally will determine soil saturation patterns and will
313 influence observed soil salinities across the marsh surface (Montalto et al. 2007). Results of
314 multiple linear regression models of cumulative regional rainfall, a driver of groundwater and
315 surface water inputs, and tide state versus our observed mean salinities in the marsh lend some
316 support to this model at our sites, with longer-term cumulative rainfall showing a greater relative
317 importance in our models than shorter-term precipitation, particularly at the PAS site. Longer-

318 term cumulative rainfall patterns may be more indicative of the magnitude of groundwater flow
319 to coastal marshes if groundwater flow in the watershed is relatively slow. However, many other
320 factors not measured or accounted for in our study, including the timing and magnitude of
321 evapotranspiration, groundwater flow patterns under a marsh, marsh topography, mean
322 temperature, and variability in tidal inundation patterns will interact to influence soil saturation
323 and observed patterns of soil salinity across a marsh.

324 In soils with similar clay and organic matter content, EC_a values will respond to changes in soil
325 composition, bulk density, moisture content, and soil salinity (Corwin and Lesch 2005).

326 Previous studies have suggested EC_a could be a reliable means to rapidly assess soil salinity,
327 particularly in hydric soils (Sheets 1994, Hanson and Kaita 1997). In homogenous, uniformly
328 saturated salt marsh soils it may be reasonable to assume that EC_a may accurately reflect changes
329 in soil salinity. However, regression statistics of the equations used to generate our calculated
330 salinity values, for example the variable correlation coefficient and slope values observed, could
331 be an indication that other soil parameters may be influencing EC_a values at our sites. Soils at
332 our sites were consistently at or around 70 % moisture, suggesting uniformly saturated soils that
333 would satisfy this assumption of the technique. We did see some intra-marsh differences in soil
334 bulk density at PAS that may have contributed somewhat to variability in EC_a values. It may also
335 be possible that our samples may have reflected spatial variation in soil composition at the sites:
336 if different regions of the marsh differed in soil composition, combining calibration data across
337 these regions may increase observed variability. Another possible explanation could be non-
338 homogeneous presence of conductive clay minerals or iron sulfate in the soils, both of which
339 may directly impact EC_a values (Laforet 2011).

340 Variability in regression statistics can also be the result of spatial variability in porewater salinity
341 values, from vagaries in water table levels or groundwater flow at our sites. For example, in our
342 study EC_a values reflected soil characteristics to 0.5 m below the marsh surface, while porewater
343 salinities used in the calibration equations were measured at a depth of 25 cm. Spatial variability
344 in soil porewater salinity either above or below our porewater sample depth would be reflected in
345 EC_a values, but not necessarily in our measured pore water salinity values. Differences in soil
346 saturation may also have influenced our measured EC_a values, although to what extent is not
347 clear. In a model of water table dynamics and groundwater movement in a tidal marsh, Ursino et
348 al. (2004) found that a zone of unsaturated, aerated soil could form in a marsh in areas away
349 from the hydraulic influence of tidal creeks, and that this aerated zone could migrate toward the
350 inner part of the marsh over time. They also found that evapotranspiration can result in the
351 formation of an unsaturated aerated layer trapped underneath saturated surface soil, particularly
352 in areas away from the influence of tidal creek hydrology (Ursino et al. 2004). Either of these
353 phenomena could impact EC_a values while conceivably not impacting measured porewater
354 salinity, and hence may contribute to the variability in calibration statistics.

355 Correlations of calculated salinity with marsh elevation supported our qualitative assessment of
356 intra-marsh salinity variation shown by the contour plots. Calculated salinity at NAR
357 significantly correlated with elevation over all the examined sample events, reinforcing observed
358 patterns of higher soil salinity near the creek edge and lower salinity towards the upland border.

359 At PAS, the lack of significant correlation may have resulted from the more homogenous salinity
360 patterns observed across the marsh surface, or may have reflected the predominance of
361 groundwater or surface freshwater inputs at the site. Interestingly, we did not consistently see a

362 significant correlation between calculated salinity and elevation despite the site having about a
363 35% greater range in elevation than NAR.

364 **Conclusions**

365 Results of our study suggest that despite variability in calibration coefficients, EC_a values reflect
366 longer-term changes in porewater salinity at a single marsh. Therefore, EC_a values show
367 promise in tracking patterns of soil salinity over time at a given site, which could aid in
368 identifying changes in marsh biogeochemistry that could ultimately impact plant zonation. For
369 example, EC_a surveys of a marsh may aid in identifying areas of irregular seawater or freshwater
370 infiltration and help increase our understanding of marsh hydrology at a given site. In addition,
371 EC_a mapping may aid in restoration planning and monitoring, especially of low-lying and
372 vulnerable coastal salt marshes. However, our results also suggest that inter-marsh comparisons
373 of EC_a values and calculated salinities should be interpreted with caution: to accurately compare
374 values, soil composition will either need to be similar, or between marsh differences adequately
375 characterized and considered during the calibration process.

376 **Acknowledgements**

377 We thank Nicole Gutierrez and Katelyn Szura for assistance with initial sample protocol
378 development, and Jara Botelho, Jess Janiec, and Tia Mitchell for assistance with data collection.
379 Cathy Wigand, Sandi Robinson, Steve Shivers and Suzy Ayvazian provided helpful input on an
380 earlier version of this manuscript. The views expressed in this paper are those of the authors and
381 do not necessarily reflect the views or policies of the US Environmental Protection Agency. This
382 contribution is identified by Tracking Number ORD-028876 of the Atlantic Ecology Division,
383 Office of Research and Development, National Health and Environmental Effects Research

384 Laboratory. Mention of trade names, products, or services does not convey, and should not be
385 interpreted as conveying, official EPA approval, endorsement, or recommendation.

386

387

388 **References**

389

390 Al Hassan M, Estrelles E, Soriano P, Lopez-Gresa MP, Belles JM, Boscaiu M, Vicente O. 2017.

391 Unraveling salt tolerance mechanisms in halophytes: a comparative study on four Mediterranean

392 *Limonium* species with different geographic distribution patterns. *Frontiers in Plant Science* 8,

393 Article No. 1438.

394

395 Barry DA, Barry SJ, Parlange JY. 1996. Capillarity correction to periodic solutions of the

396 shallow flow approximation, in *Mixing in Estuaries and Coastal Seas*, Coastal Estuarine Studies,

397 vol. 5, edited by C. Pattiaratchi, pp. 496–510, AGU, Washington, D. C.

398

399 Bricker-Urso S, Nixon SW, Cochran JK, Hirschberg DJ, Hunt C. 1989. Accretion rates and

400 sediment accumulation in Rhode Island salt marshes. *Estuaries* 12:300–317.

401

402 Burnham KP, Anderson DR. 2002. Model selection and multimodel inference: a practical

403 information-theoretic approach, 2nd edition. Springer-Verlag, New York, p. 488.

404

405 Corwin DL, Lesch SM. 2004. Apparent soil electrical conductivity measurements in agriculture.

406 *Computers and Electronics in Agriculture* 46:11–43.

407

408 DeJong E, Ballantyne AK, Cameron DR, Read DWL. 1979. Measurement of apparent electrical
409 conductivity of soils by an electromagnetic induction probe to aid salinity surveys. *Soil Science*
410 *Society of America Journal* 43:810-812.

411

412 Dodds WK. 2002. *Freshwater Ecology: Concepts and environmental applications*. Academic
413 Press, New York, 567 pp.

414

415 Doolittle J, Petersen M, Wheeler T. 2001. Comparison of two electromagnetic induction tools in
416 salinity appraisals. *Journal of Soil and Water Conservation* 56:257–262.

417

418 Geonics Limited. 2014. EM38 ground conductivity meter operating manual. Mississauga,
419 Ontario, Canada.

420

421 Hanson BR, Kaita K. 1997. Response of electromagnetic conductivity meter to soil salinity and
422 soil-water content. *Journal of Irrigation and Drainage Engineering* 123:141–143.

423

424 Hemmond HF, Fifield JL. 1982. Subsurface flow in salt marsh peat: A model and field study.

425 *Limnology and Oceanography* 27:126-136.

426

427 Kelleway JJ, Cavanaugh K, Rogers, K, Feller, Ilka C, Ens E, Doughty C, Saintilan N. 2017.

428 Review of the ecosystem service implications of mangrove encroachment into salt marshes.

429 *Global Change Biology* 23:3967-3983.

430

431 Laforet Z. 2011. Indirect measuring of soil conductivity for the calculation of pore water salinity
432 in tidal marshes. New Hampshire Sea Grant Tech 797, University of New Hampshire, Durham,
433 NH.

434

435 Li H, Jiao JJ. 2003. Influence of the tide on the mean watertable in an unconfined, anisotropic,
436 inhomogeneous coastal aquifer. *Advances in Water Resources* 26:9-16.

437

438 Montalto FA, Parlange JY, Steenhuis TS. 2007. A simple model for predicting water table
439 fluctuations in a tidal marsh. *Water Resources Research* 43:W03439,
440 doi:10.1029/2004WR003439.

441

442 Moore GE, Burdick DM, Peter CR, Keirstead DR. 2011. Mapping soil pore water salinity of
443 tidal marsh habitats using electromagnetic induction in Great Bay Estuary, USA. *Wetlands*
444 31:309-318.

445

446 Paine JG, White WA, Smyth RC, Andrews JR, Gibeaut JC. 2004. Mapping coastal environments
447 with lidar and EM on Mustang Island, Texas, U.S. *The Leading Edge Summer*: 894–898.

448

449 Parlange JY, Stagnitti F, Starr JL, Braddock RD. 1984. Free-surface flow in porous media and
450 periodic solution of the shallow flow approximation. *Journal of Hydrology* 70:251–263.

451

452 Portnoy JW, Valiela I. 1997. Short-term effects of salinity reduction and drainage on salt-marsh
453 biogeochemical cycling and *Spartina* (cordgrass) production. *Estuaries* 20:569–578.

454

455 Robinson DA, Lebron I, Lesch SM, Shouse P. 2004. Minimizing drift in electrical conductivity
456 measurements in high temperature environments using the EM-38. *Soil Science Society of*
457 *America Journal* 68:339-345.

458

459 Sheets KR, Taylor JP, Hendrickx JMH. 1994. Rapid salinity mapping by electromagnetic
460 induction for determining riparian restoration potential. *Restoration Ecology* 2:242–246.

461

462 Silvestri S., Marani M. 2004. Salt-marsh vegetation and morphology: basic physiology,
463 modelling and remote sensing observations. Pages 1-21 in ‘Ecogeomorphology of Tidal
464 Marshes’,: S. Fagherazzi, L. Blum, Marani M, Eds., American Geophysical Union, Coastal and
465 Estuarine Monograph Series, 2004.

466

467 Smith SM, Tyrrell M, Medeiros K, Bayley H, Fox S, Adams M, Mejia C, Dijkstra A, Janson S,
468 Tanis M. 2017. Hypsometry of Cape Cod salt marshes (Massachusetts, U.S.A.) and predictions
469 of marsh vegetation responses to sea-level rise. *Journal of Coastal Research* 33:537-547.

470

471 Turner RE, Swenson EM, Milan CS. 2000. Organic and inorganic contributions to vertical
472 accretion in salt marsh sediments. In: Weinstein MP, Kreeger DA (eds.), *Concepts and*
473 *Controversies in Tidal Marsh Ecology*. Dordrecht, The Netherlands: Springer, pp. 583–595.

474

475 Ursino N, Silvestri S, Marani M. 2004 Subsurface flow and vegetation patterns in tidal
476 environments. *Water Resources Research* 40:W05115, doi:10.1029/2003WR002702.

477

478 Watson EB, Wigand C, Davey EW, Andrews HM, Bishop J, Raposa KB. 2017. Wetland loss
479 patterns and inundation-productivity relationships prognosticate widespread salt marsh loss for
480 southern New England. *Estuaries and Coasts* 40:662-681.

481

Table 1 (on next page)

Mean whole-marsh conductivity, pore water salinity, calculated salinity, and regression coefficients for 24 sample events at the a) southern (NAR) and b) northern (PAS) study sites.

Conductivity and calculated salinity were averaged across all sample points on the marsh surface, and measured pore water salinity was averaged across the sub-set of sample points where pore water was collected. Calibration coefficients for the corresponding calibration curves were constructed from a least-squares regression of apparent conductivity (EC_a) values and measured pore water salinities.

1 a.)

NAR Sample Date	Mean Conductivity (mS m⁻¹)	Mean Measured Pore Water Salinity (ppt)	Mean Calculated Salinity (ppt)	Calibration Coefficient (r²)
10/30/2015	317.7 ± 24.5	24.3 ± 4.0	23.4 ± 1.5	0.78
12/4/2015	238.4 ± 18.8	25.1 ± 2.9	26.2 ± 1.3	0.56
12/30/2015	249.4 ± 21.4	23.7 ± 3.1	24.5 ± 1.0	0.46
1/29/2016	222.7 ± 20.5	25.6 ± 2.4	24.7 ± 0.8	0.16
3/7/2016	213.6 ± 20.2	22.8 ± 3.8	18.2 ± 1.6	0.66
4/6/2016	191.6 ± 17.8	21.4 ± 2.3	21.5 ± 0.8	0.13
5/4/2016	193.6 ± 18.3	20.0 ± 2.5	16.3 ± 0.9	0.25
6/1/2016	261.5 ± 24.3	15.9 ± 3.8	17.7 ± 1.6	0.92
6/24/2016	305.7 ± 23.2	22.7 ± 2.3	20.3 ± 1.0	0.63
8/4/2016	402.6 ± 21.9	34.0 ± 2.0	33.9 ± 1.3	0.44
9/16/2016	389.0 ± 21.6	36.1 ± 1.3	35.4 ± 0.4	0.27
10/7/2016	388.1 ± 18.0	34.4 ± 1.3	34.6 ± 1.1	0.61
10/28/2016	386.7 ± 19.4	35.3 ± 1.4	35.2 ± 1.0	0.42
12/1/2016	491.5 ± 33.9	32.7 ± 1.4	31.2 ± 1.1	0.41
12/30/2016	263.1 ± 20.2	29.6 ± 2.3	28.8 ± 1.0	0.37
1/29/2017	269.6 ± 16.9	28.8 ± 2.7	27.1 ± 1.2	0.41
3/2/2017	252.2 ± 19.4	21.3 ± 2.4	22.6 ± 1.3	0.66
3/29/2017	253.0 ± 22.5	23.5 ± 2.1	23.1 ± 1.0	0.37
5/3/2017	245.0 ± 16.9	24.7 ± 1.9	23.0 ± 1.0	0.36
6/15/2017	295.7 ± 20.7	21.6 ± 2.1	21.3 ± 0.9	0.44
7/21/2017	347.8 ± 19.4	26.6 ± 2.1	24.9 ± 1.2	0.77
8/16/2017	353.9 ± 18.4	27.9 ± 1.9	26.7 ± 0.9	0.51
9/14/2017	381.3 ± 16.8	27.0 ± 2.1	27.6 ± 0.9	0.67
10/27/2017	339.4 ± 18.6	30.5 ± 1.5	30.2 ± 1.0	0.54

2

3

4 b.)

PAS Sample Date	Mean Conductivity (mS m⁻¹)	Mean Measured Pore Water Salinity (ppt)	Mean Calculated Salinity (ppt)	Calibration Coefficient (r²)
10/30/2015	249.7 ± 9.5	20.5 ± 2.0	21.3 ± 1.0	0.72
12/4/2015	207.7 ± 7.5	21.9 ± 1.4	22.4 ± 0.9	0.12
12/30/2015	193.8 ± 7.6	16.6 ± 2.8	16.7 ± 1.2	0.58
1/29/2016	176.7 ± 7.8	15.1 ± 1.3	14.7 ± 1.1	0.31
3/7/2016	151.7 ± 6.4	11.9 ± 1.3	17.4 ± 0.7	0.53
4/6/2016	146.9 ± 6.7	10.9 ± 1.6	11.4 ± 1.0	0.34
5/4/2016	154.1 ± 6.7	8.7 ± 1.3	8.3 ± 0.5	0.33
6/1/2016	183.2 ± 7.3	9.1 ± 1.4	8.6 ± 0.5	0.13
6/24/2016	227.8 ± 8.7	14.4 ± 1.7	16.8 ± 0.8	0.01
8/4/2016	272.4 ± 9.7	22.5 ± 1.8	23.7 ± 1.6	0.65
9/16/2016	301.9 ± 10.9	26.7 ± 1.0	26.2 ± 1.4	0.19
10/7/2016	296.7 ± 8.6	23.3 ± 1.4	23.7 ± 1.3	0.42
10/28/2016	251.1 ± 7.3	25.6 ± 0.8	25.3 ± 1.1	0.29
12/1/2016	233.7 ± 5.9	21.8 ± 1.0	22.0 ± 1.1	0.28
12/30/2016	178.5 ± 6.1	22.3 ± 1.3	22.3 ± 1.3	0.59
1/29/2017	172.5 ± 5.6	18.2 ± 1.5	18.9 ± 0.9	0.20
3/2/2017	186.2 ± 8.5	13.7 ± 1.2	14.1 ± 0.8	0.29
3/29/2017	168.9 ± 6.2	17.6 ± 1.6	17.3 ± 0.9	0.52
5/3/2017	157.7 ± 6.9	14.7 ± 2.2	20.0 ± 1.3	0.59
6/15/2017	199.1 ± 8.4	10.6 ± 1.3	12.3 ± 0.7	0.75
7/21/2017	194.4 ± 7.1	9.0 ± 0.5	9.1 ± 0.4	0.13
8/16/2017	240.4 ± 6.6	12.7 ± 1.1	13.2 ± 0.6	0.16
9/14/2017	274.3 ± 6.6	18.4 ± 1.0	18.1 ± 0.7	0.52
10/27/2017	263.0 ± 6.1	21.4 ± 1.5	21.1 ± 1.0	0.59

5

Table 2 (on next page)

Best predictive models incorporating the effect of cumulative rainfall amounts and tide state on calculated salinity values at the a) southern (NAR) and b) northern (PAS) study sites.

Models best supported by the data, or those having ΔAIC_c values between 0.00 and 2.00, are listed.

1 a.)

NAR Model^a	R²	AIC_c	ΔAIC_c^b
48.77 – 0.831(6 MON) – 3.193(TIDE)	0.55	69.12	0.00
44.22 – 0.781(6 MON)	0.48	70.13	1.01
47.54 – 0.873(6 MON) – 3.124(TIDE) + 0.531(1 MON)	0.57	70.78	1.66

2

3 b.)

PAS Model^a	R²	AIC_c	ΔAIC_c^b
37.41 – 0.873(6 MON) – 3.124(TIDE) + 0.531(1 MON)	0.80	50.55	0.00

4

5 ^a1 MON = cumulative rainfall 30 days prior to sample event; 6 MON = cumulative rainfall 180
6 days prior to sample event; TIDE = tide state.

7 ^bΔAIC_c = AIC_{ci} - AIC_{cmin}

8

Table 3(on next page)

Relative importance of rainfall and tide parameters in regression models explaining calculated salinity values during 24 sample events at the southern (NAR) and northern (PAS) study sites.

24 HR = cumulative rainfall 24 hours prior to sampling event; 1 MON = cumulative rainfall 30 days prior to sample event; 6 MON = cumulative rainfall 180 days prior to sample event; TIDE = tide state.

1

Parameter	NAR Relative Importance	PAS Relative Importance
24 HR	0.195	0.188
1 MON	0.327	0.999
6 MON	1.000	1.000
TIDE	0.596	0.966

2

Table 4(on next page)

Mean bulk density and percent moisture in soil samples to 25 cm depth collected in high, mid, and low marsh locations at the a) southern (NAR) and b) northern (PAS) study sites.

1

Site	Location	Bulk Density (g cm⁻³)	Percent Moisture (%)
NAR	High marsh	0.31 ± 0.04	71.3 ± 3.3
NAR	Mid marsh	0.19 ± 0.01	84.3 ± 1.4
NAR	Low marsh	0.34 ± 0.29	69.0 ± 16.8
PAS	High marsh	0.24 ± 0.05	77.1 ± 0.6
PAS	Mid marsh	0.17 ± 0.02	84.2 ± 1.4
PAS	Low marsh	0.16 ± 0.03	83.2 ± 2.4

2

Table 5 (on next page)

Least squares regression statistics for the relationship between calculated salinity and elevation at the a) NAR and b) PAS.

1 a.)

<i>NAR Minima</i>				
Sample Date	Slope	R²	Degrees of Freedom	p
4/6/2016	-8.42	0.35	44	< 0.001
5/4/2016	-25.47	0.54	52	< 0.001
6/1/2016	-38.62	0.42	34	< 0.001
6/15/2017	-21.72	0.55	58	< 0.001
7/21/2017	-36.09	0.59	60	< 0.001
8/16/2017	-24.99	0.63	61	< 0.001
<i>NAR Maxima</i>				
Sample Date	Slope	R²	Degrees of Freedom	p
9/16/2016	-11.90	0.61	47	< 0.001
10/7/2016	-15.56	0.57	52	< 0.001
10/28/2016	-9.75	0.33	54	< 0.001
9/14/2017	-27.62	0.53	76	< 0.001
10/27/2017	-18.05	0.57	54	< 0.001
11/21/2017	-24.68	0.55	61	< 0.001

2

3 b.)

<i>PAS Minima</i>				
Sample Date	Slope	R²	Degrees of Freedom	p
4/6/2016	0.71	0.01	25	0.643
5/4/2016	-0.34	0.01	30	0.556
6/1/2016	-0.67	0.07	30	0.149
6/15/2017	-4.10	0.37	36	< 0.001
7/21/2017	0.03	0.01	29	0.897
8/16/2017	-1.11	0.20	33	0.007
<i>PAS Maxima</i>				
Sample Date	Slope	R²	Degrees of Freedom	p
9/16/2016	-0.25	0.00	25	0.746
10/7/2016	-4.54	0.34	30	< 0.001
10/28/2016	0.89	0.07	31	0.124
9/14/2017	-1.51	0.12	39	0.024
10/27/2017	-0.51	0.01	33	0.601
11/21/2017	-0.11	0.00	35	0.907

Figure 1

Location of the two salt marshes study sites Narrow River marsh (NAR) and Passeonkquis marsh (PAS) in the Narragansett Bay estuary, Rhode Island, USA.

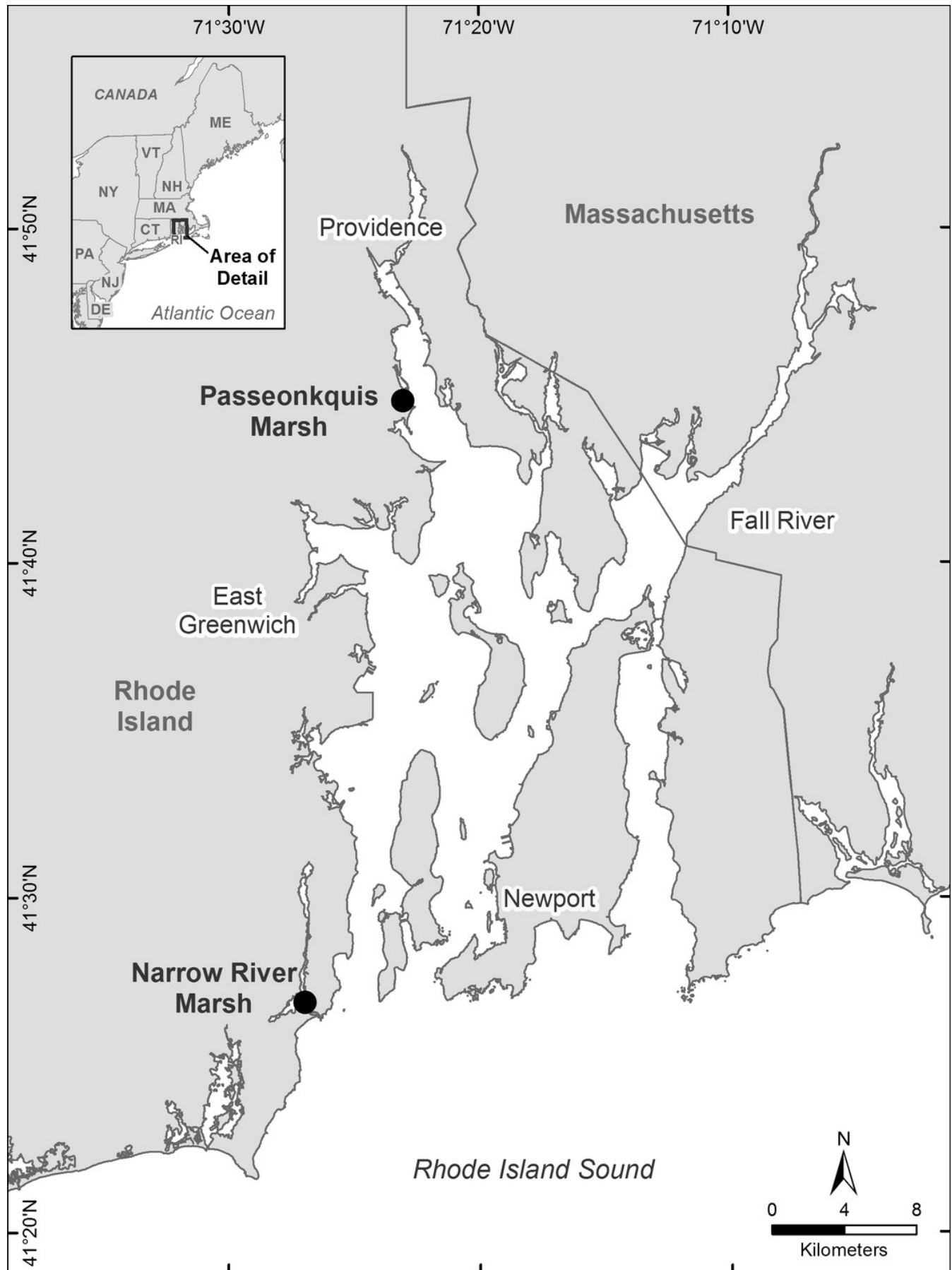
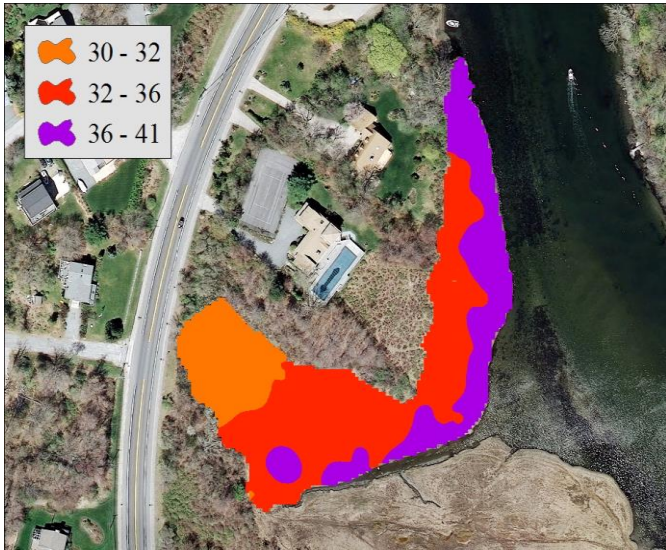


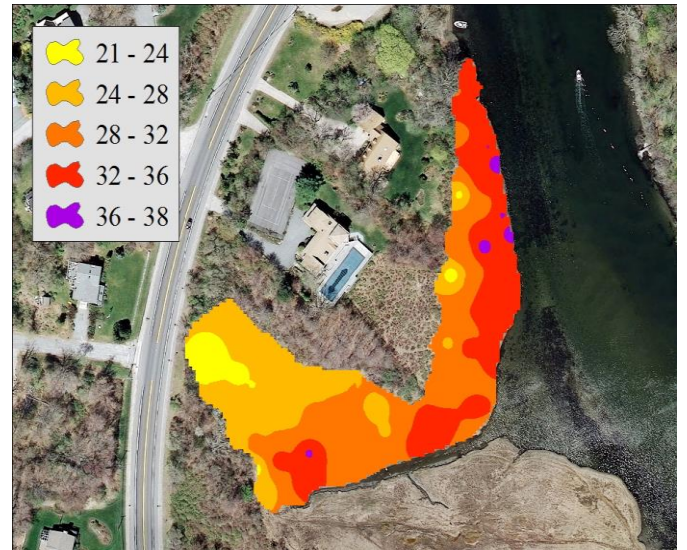
Figure 2 (on next page)

Contour plots of calculated salinity across the marsh surface of NAR corresponding to the a.) mean calculated salinity maxima and b.) mean calculated salinity minima.

a)

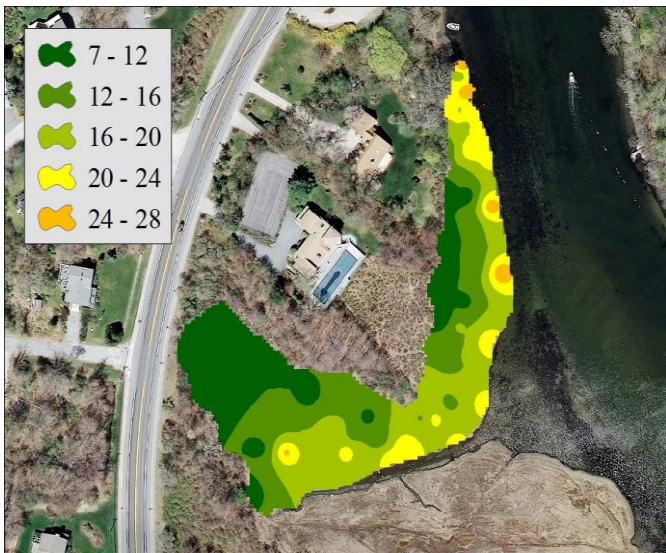


September 16, 2016

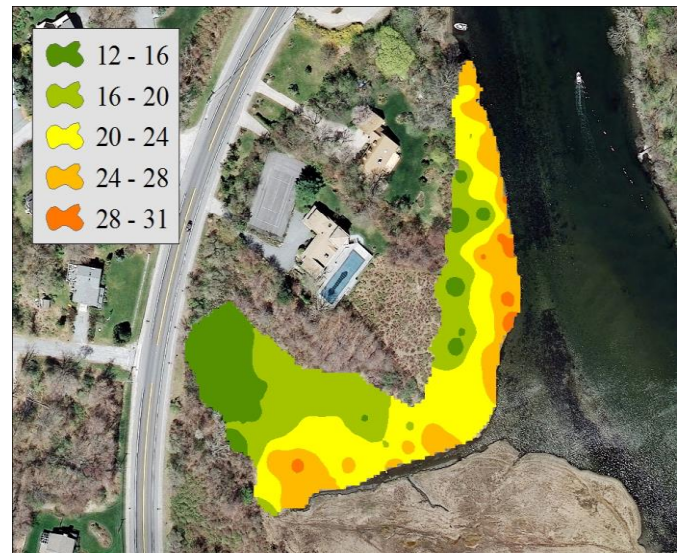


October 27, 2017

b)



May 4, 2016

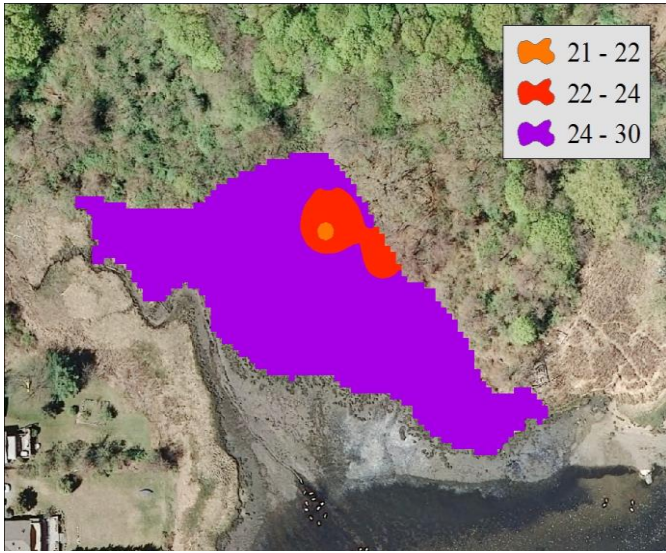


June 15, 2017

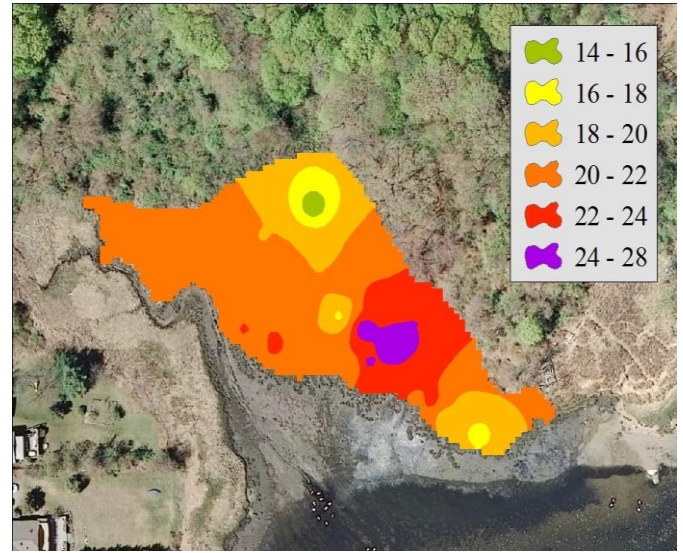
Figure 3 (on next page)

Contour plots of calculated salinity across the marsh surface of PAS corresponding to the a.) mean calculated salinity maxima and b.) mean calculated salinity minima.

a)

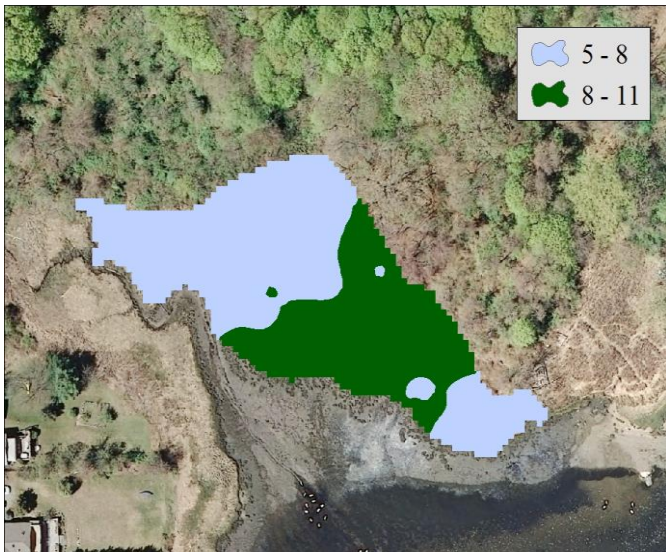


September 16, 2016



October 27, 2017

b)



May 4, 2016



July 21, 2017

Figure 4(on next page)

Plot of mean whole-marsh calculated salinity versus day of sampling for the NAR and PAS study sites.

The date of the initial sample event October 30, 2015 was designated as day 1. Sample minima at days 188 and 631 corresponded to the dates May 4, 2016 and July 21, 2017. Sample maxima at days 323 and 729 corresponded to the dates September 16, 2016 and October 27, 2017.

